Biomaterials 31 (2010) 577–584

Contents lists available at ScienceDirect

Biomaterials

journal homepage: www.elsevier.com/locate/biomaterials

A microfabricated platform for high-throughput unconfined compression of micropatterned biomaterial arrays

Christopher Moraes [a,b], GongHao Wang [a], Yu Sun [a,b,**], Craig A. Simmons [a,b,c,*]

[a] Department of Mechanical and Industrial Engineering, University of Toronto, 5 King's College Road, Toronto, Ontario, M5S 3G8, Canada
[b] Institute of Biomaterials and Biomedical Engineering, University of Toronto, 164 College Street, Toronto, Ontario M5S 3G9, Canada
[c] Faculty of Dentistry, University of Toronto, 124 Edward Street, Toronto, Ontario M5G 1G6, Canada

ARTICLE INFO

Article history:
Received 3 September 2009
Accepted 16 September 2009
Available online 9 October 2009

Keywords:
Hydrogel
Micropatterning
Biomaterial arrays
High-throughput
Mechanical stimulation
Compression

ABSTRACT

High-throughput screening techniques for cellular response are often unable to account for several factors present in the *in vivo* environment, many of which have been shown to modulate cellular response to the screened parameter. Culture in three-dimensional biomaterials and active mechanical stimulation are two such factors. In this work, we integrate these microenvironmental parameters into a versatile microfabricated device, capable of simultaneously applying a range of cyclic, compressive mechanical forces to cells encapsulated in an array of micropatterned biomaterials. The fabrication techniques developed here are broadly applicable to the integration of three-dimensional culture systems in complex multilayered polymeric microdevices. Compressive strains ranging from 6% to 26% were achieved simultaneously across the biomaterial array. As a first demonstration of this technology, nuclear and cellular deformation in response to applied compression was assessed in C3H10T1/2 mouse mesenchymal stem cells encapsulated within poly(ethylene glycol) hydrogels. Biomaterial, cellular, and nuclear deformations were non-linearly related. Parametric finite element simulations suggested that this phenomenon was due to the relative stiffness differences between the hydrogel matrix and that of the encapsulated cell and nucleus, and to strain stiffening of the matrix with increasing compression. This complex mechanical interaction between cells and biomaterials further emphasizes the need for high-throughput approaches to conduct mechanically active experiments in three-dimensional culture.

1. Introduction

High-throughput screening (HTS) has been a critical technology in driving drug discovery, tissue engineering and fundamental cell biology research [1]. However, these techniques are hindered by the failure of standard HTS platforms to account for a number of factors present in the *in vivo* cellular microenvironment [2]. Technological progress in microfabricated systems has enabled the simulation of complex cellular environments, while maintaining the arrayed format suitable for systematic HTS. Currently, factors such as chemical stimulation [3], the extracellular matrix [4–6] and cell-biomaterial interactions [7] can be precisely manipulated. However, HTS techniques for drug discovery, biomaterial development, and tissue engineering require the inclusion and manipulation of other parameters to better recreate a more realistic *in vivo* environment.

One such parameter is the dimensionality of the culture system. Three-dimensional cell culture has been shown to significantly impact cell function [8,9], and is a core approach in tissue engineering to produce functional tissue replacements [10,11]. Three-dimensional culture has also been shown to modulate cellular response to chemical factors in the microenvironment [12–14], suggesting that biomolecular screens must incorporate this aspect of dimensionality to produce clinically relevant results [15]. Advances in biomaterial technologies have enabled spatial definition of three-dimensional structures for tissue engineering [16–18], and these approaches have only recently enabled high-throughput screening in three-dimensional culture systems [19,20].

Dynamic mechanical forces also play a role in driving cell function *in vivo* [21,22]. Many cells are exquisitely sensitive to applied mechanical stimulation in both two- and three-dimensional environments [23,24]. Mechanical forces modulate cellular response to other stimuli [25–27], and are often used to encourage appropriate cell growth and function in engineered tissues [28]. For example, dynamic compression has been shown to regulate chondrocyte apoptosis in cartilage explants [29]; chondrocyte matrix biosynthesis [30]; intervertebral disc cell gene and protein expression [31]; bone

* Corresponding author. Department of Mechanical and Industrial Engineering, University of Toronto, 5 King's College Road, Toronto, Ontario, M5S 3G8, Canada Tel.: +1 416 946 0548; fax: +1 416 978 7753.
** Corresponding author. Tel.: +1 416 946 0549; fax: +1 416 978 7753.
E-mail addresses: sun@mie.utoronto.ca (Y. Sun), simmons@mie.utoronto.ca (C.A. Simmons).

0142-9612/$ – see front matter © 2009 Elsevier Ltd. All rights reserved.
doi:10.1016/j.biomaterials.2009.09.068

homeostasis [32]; and stem cell chondrogenesis [33], osteogenesis [34] and adipogenesis [35]. Compression has also been shown to modulate cellular response to other stimuli [36], and thus has potential in making HTS assays more suitable to clinically-relevant applications.

Creating a range of mechanically dynamic compressive microenvironments in three-dimensional culture is challenging with conventional equipment and techniques. To realize mechanically active HTS arrays, this paper reports on the incorporation of an aligned photopolymerized biomaterial array, stably micropatterned within a multilayer polydimethylsiloxane (PDMS) microfabricated platform. This integration of biomaterial and microfabrication technologies results in a microdevice capable of simultaneously and systematically varying compressive strain levels across an array of three-dimensional, cell-laden biomaterial microconstructs.

As a first demonstration of the functionality of this system, an array of poly(ethylene glycol) (PEG) biomaterial microconstructs containing mouse mesenchymal stem cells were simultaneously compressed to varying degrees. Cellular deformation resulting from the applied mechanical stimulation was measured via fluorescent confocal microscopy, in order to rapidly assess the minimum levels of strain required to cause cellular deformation. A parametric finite element model was used to further probe and provide a potential explanation for the observed nonlinearity in cellular deformation.

2. Materials and methods

Unless otherwise stated, all chemicals and reagents for cell culture were purchased from Sigma–Aldrich (Oakville, ON, Canada); fluorescent dyes from Invitrogen (Burlington, ON, Canada); and all other equipment and materials from Fisher Scientific Canada (Ottawa, ON, Canada).

2.1. Hydrogel chemistry

Hydrogel arrays were produced by mask-based photolithography of a cell suspension in a PEG precursor [37]. Poly (ethylene glycol) diacrylate (PEGDA) with a molecular weight of 3.4 kDa was purchased from Laysan Bio (Arab, AL, USA). A hydrogel precursor solution consisting of 10% w/v PEGDA and 10% w/v PEG (8 kDa) in unsupplemented Eagle's Buffered Media (EBM) was prepared. Irgacure 2959 (Ciba Specialty Chemicals; Tarrytown, NY, USA) was dissolved in 1-vinyl-2-pyrolidone (100 mg/mL) to form a photoinitiator stock solution. This stock solution was then added to the hydrogel precursor solution to a concentration of 0.4% w/v of photoinitiator. The precursor solution was vortexed thoroughly and passed through a 0.45 μm syringe filter, before being mixed in a 1:1 ratio with either unsupplemented EBM or a suspension of C3H10T1/2 mouse mesenchymal stem cells (ATCC, Manassas, VA; 8×10^6 cells/mL for viability studies and 2×10^6 cells/mL for compression experiments), depending on the experimental conditions required.

2.2. Device fabrication

The PDMS device consists of 25 vertically actuated loading posts, arranged in a 5×5 array to produce five replicates of five distinct mechanical conditions (Fig. 1). The device pitch is based on a 1536-well plate. The array of loading posts is suspended over actuation cavities of varying diameters, and posts are raised by applying pressure beneath the suspended membranes via an integrated network of channels in the PDMS device (Fig. 2). A solenoid valve (Pneumadyne; Plymouth, MN, USA) was used to apply a step pressure of 55 kPa generated by an eccentric diaphragm pump (SP 500 EC-LC; Schwarzer Precision; Germany). By varying the diameters of the actuation cavities, a single pressure source can be used to create a range of vertical displacements across the array.

Devices were fabricated using Sylgard 184 PDMS kits (Dow Corning, purchased through A.E. Blake Sales Ltd.; Toronto, ON, Canada) using sandwich mold fabrication [38] to prevent alignment registration errors between multiple device layers [39]. Briefly, a layer of PDMS was cured while compressed between an SU-8 patterned glass master and a transparency film (Grand & Toy; Toronto, ON, Canada). The patterned PDMS layers preferentially adhere to the transparency, from where they can be bonded and transferred to a $3'' \times 2''$ glass slide, or another patterned PDMS layer. A series of cross-shaped marks was fabricated directly into the PDMS device to facilitate alignment with corresponding marks on the photopolymerization mask. To reduce the gas permeability of the PDMS device, a layer of Parylene-C was deposited using a PDS 2010 Labcoter® 2 system (Specialty Coating Systems; Indianapolis, IN, USA). Clear tape was used to mask the device around the post array, before a 1 μm thick conformal layer of Parylene-C was deposited over the surface. Peeling the tape away removed the Parylene film from the device periphery.

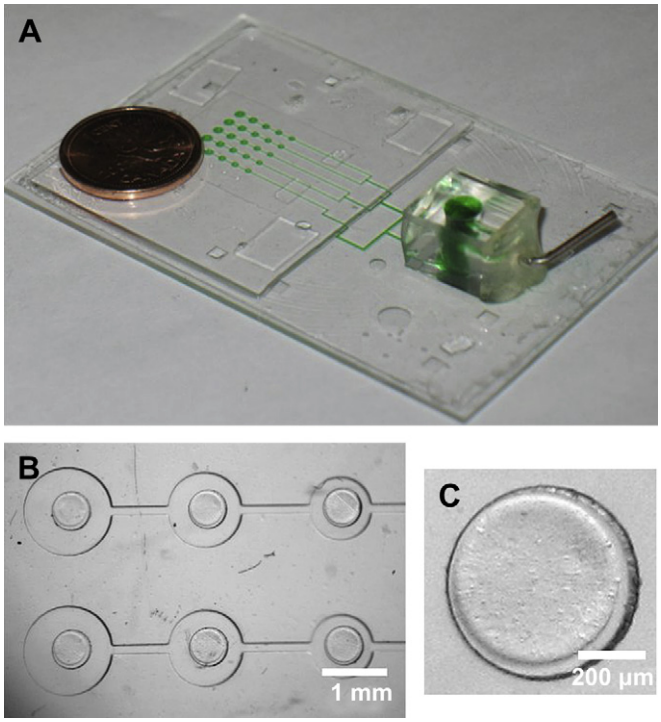

Fig. 1. (A) Microfabricated device with a 5×5 array of mechanically active three-dimensional culture sites (green dye in the pressurized actuation channels). (B) Increasing actuation cavity size across the array enables a range of mechanical conditions to be created simultaneously. (C) Cylindrical hydrogel polymerized on a loading post in the mechanically active culture array.

A 200 μm thick slab of PDMS was cast in a Petri dish, and small sections of this slab were bonded as spacers between the multilayer device and a glass coverslip (Fig. 2), creating a thin polymerization chamber above the loading posts. The coverslip was functionalized by treatment with a 2% v/v solution of 3-(trimethoxysilyl) propyl methacrylate [40] to provide binding sites for the polymerized hydrogels.

A connector was then attached to the actuation cavity network. Imaging the encapsulated cells was found to be severely hampered by the formation of condensate droplets in the actuation cavities of the device during the course of the experiment. In order to prevent this, the actuation cavities were backfilled with deionized water, prior to further fabrication steps.

2.3. Hydrogel lithography

A fluorescent microscope light source (X-Cite 120, EXFO Life Sciences; Mississauga, ON, Canada) was modified to provide UV illumination. The fiber optic guide and microscope adapter were removed from the fluorescent microscope, and set up in a custom-made vertical polymerization system. The broad-spectrum source was passed through a 365 nm narrow band filter (removed from a BlakRay illumination lamp; UVP; Ottawa, ON, Canada) and a manual shutter system, to illuminate a removable lift stage. The stage was raised towards the light source, such that the incident UV dose to the device was 17.5 mW/cm^2 (measured using a 365 nm intensity meter), with negligible variation in intensity over a 2 cm $\times$ 2 cm area.

The cell suspension and hydrogel precursor mixture were injected into the polymerization chamber using a long 25-gauge needle (Fig. 2B). Care was taken to ensure that no air bubbles were trapped within the chamber. Enough fluid was injected to ensure that the edges of the polymerized array were at least 1 cm away from the air-fluid boundary.

A printed transparent film (CAD/Art Services; Bandon, OR, USA) was used to selectively photopolymerize the hydrogel. Arrayed circular patterns (500 μm in diameter) were used for all experiments. The mask was placed on the device surface. Alignment was manually conducted with the aid of a Navitar 12× zoom vision system (Navitar; Rochester, NY, USA). The stage was then illuminated with UV light, selectively polymerizing the hydrogel.

The arrays were washed three times by injecting sterile EBM into the device chamber to displace the unpolymerized precursor solution. For those experiments

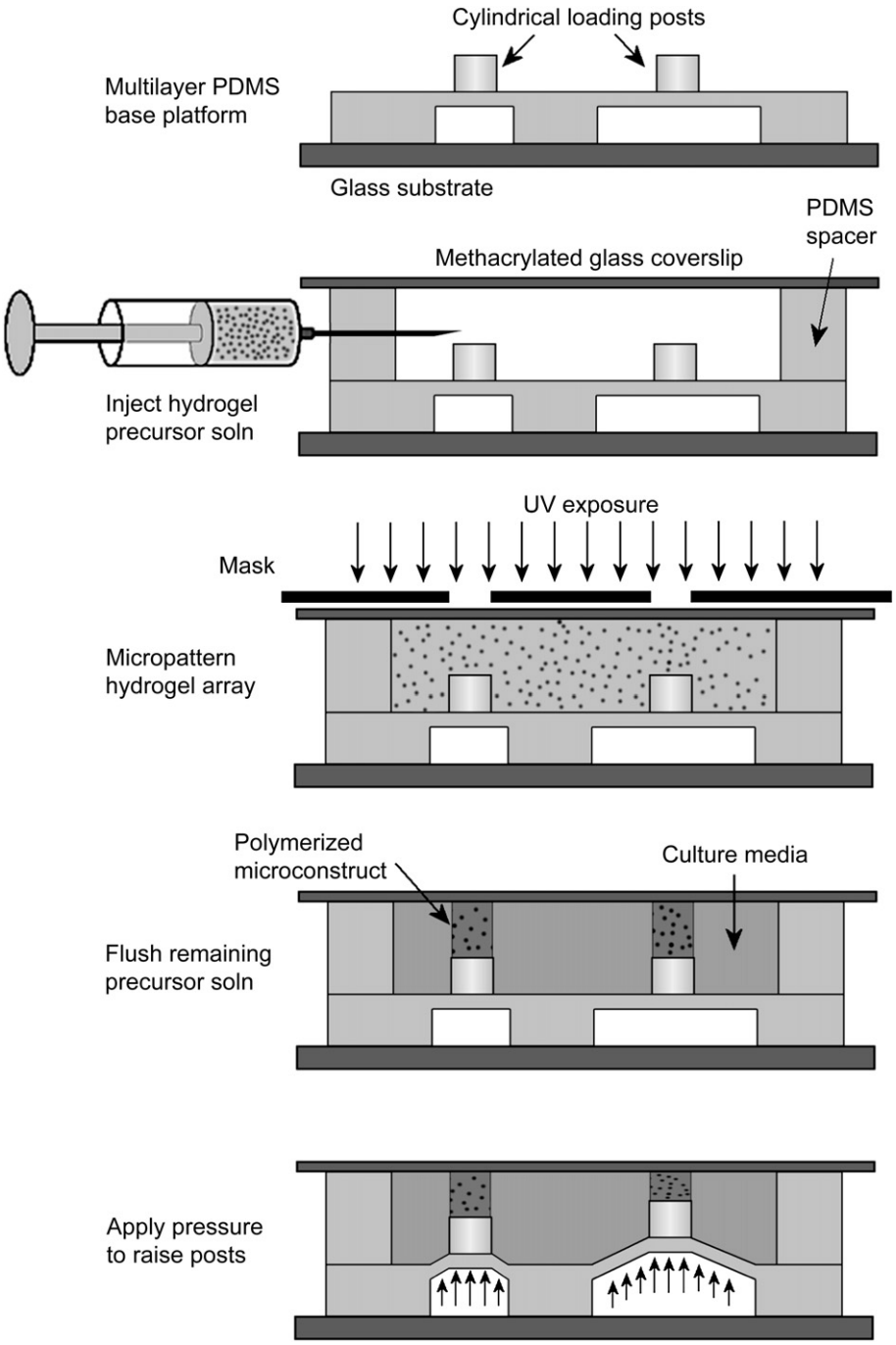

Fig. 2. Fabrication process for mechanically active three-dimensional cell culture arrays.

with encapsulated cells, devices were incubated (37 °C, 5% CO_2) for at least 1 h before fluorescent staining and mechanical compression.

2.4. Characterization of PEG polymerization

In order to investigate the effects of microdevice materials on hydrogel microconstruct formation, the photopolymerization procedure was conducted on multiple substrates. As with device fabrication, a PDMS spacer was bonded between methacrylated glass coverslips and three substrate materials: bare glass, PDMS and Parylene-coated PDMS, to create polymerization chambers of different materials. An additional oxygen-depleted PDMS substrate was created by placing a PDMS-based chamber under vacuum (Savant VLP80 rotary vacuum pump) for 20 min immediately prior to polymerization. Photopolymerized arrays were imaged under a stereoscope (Olympus; Markham, ON, Canada). A standard binary threshold level was applied in ImageJ (NIH), and automated ellipse fitting algorithms were used to measure the dimensions of the polymerized hydrogels across the area of interest.

2.5. Fluorescent staining and microscopy

Microconstruct deformation was assessed by mixing 1 μm diameter FITC fluorescent beads (Bangs Laboratories; Fishers, IN, USA) into the hydrogel solution before polymerization. Confocal microscopy (Fluoview 300, Olympus) was used to collect three-dimensional images of each hydrogel cylinder when at rest and when the device was actuated, at a magnification of $10\times$ ($n = 3$).

Cell viability in the polymerized arrays was assessed using a calcein AM and ethidium homodimer LIVE/DEAD cytotoxicity assay. To measure cytoplasmic and nuclear deformation in response to mechanical stimulation, cells were stained with calcein AM and DRAQ5 nuclear stain. The use of calcein AM served the dual purpose of

staining the cellular cytoplasm and ensuring that the particular cell under study was viable. Confocal images were collected at 40× magnification for each of the five mechanical conditions across the array, when the hydrogels were at rest and under compression.

2.6. Image analysis

Confocal images were processed using a semi-automated macro in ImageJ. For the fluorescent bead characterization studies, the confocal image stacks were resliced orthogonal to the principal axis of the hydrogel cylinders. A z-projection of the resliced stack was taken, the heights of the cylinders under compression were measured, and the percentage changes in cylinder height were calculated.

In order to assess cellular and nuclear deformation under compression, a synchronized selection function was used to crop a separate image stack for each isolated cell in the photopolymerized cylinder, when at rest and when compressed. There were at least three cells in each image stack which were physically separate from other cells in the microconstruct. The stacks were then resliced orthogonally, and a z-projection of the stacks was applied to clearly define the outlines of the cytoplasm and nuclei. A threshold binary function was applied and ellipses were fitted to the cross-sectional view of the cells and nuclei when at rest and when under compression.

A mathematical descriptor for 'nuclear shape' and 'cell shape' was defined as the aspect ratio between the x- and y-axes of the fitted ellipse. 'Cellular deformation' and 'nuclear deformation' were defined as the ratios between the normal and compressed aspect ratios of the cells and nuclei. Deformation values for all the single cells within a hydrogel cylinder were averaged. These values were used to obtain a mean and standard deviation across three cylinders under similar mechanical conditions.

2.7. Statistical analysis

All statistical analyses were performed using SigmaStat 3.5 (Systat Software Inc.; San Jose, CA, USA). One-way ANOVA tests were used to compare groups, and post-hoc comparisons were conducted using the Tukey method. Graphical results are reported as means ± standard deviation.

2.8. Finite element simulations

In order to assess the impact of the relative differences in stiffness between the hydrogel and the encapsulated cell on cellular deformation, finite element simulations were conducted in ANSYS (ANSYS Inc.; Canonsburg, PA, USA). An axisymmetric, large displacement model of a cell embedded within a hydrogel was developed using quadrilateral PLANE183 elements. The simulations were designed to be first-order approximations to this problem, and assumed isotropic linear elastic behaviour of the cell and the surrounding matrix. The matrix was defined as a 500 μm diameter cylinder, 100 μm in height, encapsulating a 20 μm diameter sphere, representing the cell. The cell was assumed to be fixed in the matrix, such that no slippage occured between the two interacting surfaces. The standard ANSYS mesh generator algorithm was used to create a mesh with 932 elements in the cell, and 6180 elements in the hydrogel microconstruct. The relative modulus between the two materials (E^*_{matrix}) was varied over seven orders of magnitude, and fixed deformation constraints were applied to the matrix to produce compressions of 1%, 5% and 10%. The resulting change in aspect ratio was determined for values of E^*_{matrix} ranging from 0.001 to 1000.

3. Experimental results

3.1. Hydrogel integration and characterization

The materials used to fabricate the polymerization chamber played a significant role in PEG polymerization kinetics. The feature sizes of micropatterned hydrogel constructs were used to assess the degree of polymerization on various substrate materials commonly used in microfabricated devices. A significant reduction in microstructure diameters was observed on all PDMS substrates as compared to the glass substrate, even with a 2.5-fold increase in UV exposure time ($p < 0.05$; Fig. 3). Depleting the oxygen levels in the PDMS substrate improved polymerization kinetics, but these results varied from experiment to experiment. Coating the PDMS surface with a thin conformal layer of Parylene-C consistently resulted in hydrogel features comparable to those produced on bare glass.

The viability of the encapsulated C3H10T1/2 cells was found to decrease significantly at polymerization times greater than 300 s (data not shown). Since the time required for complete hydrogel polymerization on the PDMS device substrates was well in excess of 300 s, PDMS microdevices used in this study were coated with a 1 μm layer of Parylene-C to minimize exposure time and maintain cell viability. The critical parameters for accurate reproduction of PEG microstructures in the Parylene-coated PDMS microdevices were exposure time and intensity. For cylindrical hydrogel constructs 500 μm in diameter, an exposure time of 195 s at 17.5 mW/cm^2 was found to accurately replicate the mask pattern, and obtain an initial cell viability of 69.4 ± 3.4%, which is comparable to viabilities achieved in this biomaterial in other micropatterning studies [41]. Microconstruct diameters were similar across the 1 cm^2 area of the array for our polymerization system.

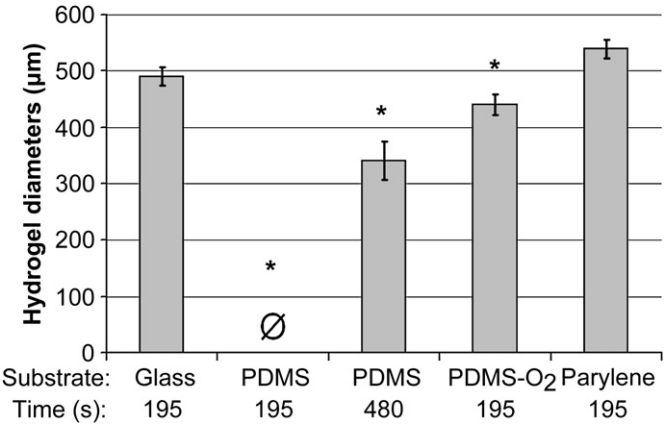

Fig. 3. Micropatterning of hydrogel arrays on various materials used in microfabrication. The diameters across an array of hydrogel cylinders were measured on glass, PDMS, oxygen-depleted PDMS and Parylene substrates, for two UV exposure times. Polymerization on the Parylene and glass substrates for the same exposure time was not significantly different, whereas hydrogel features on all other conditions were undersized (*$p < 0.05$ as compared to polymerization on the glass substrate).

3.2. Microconstruct compression

Micropatterned PEG arrays were successfully integrated into the Parylene-coated PDMS devices, confirmed by direct visual observation (Fig. 1C) and confocal microscopy (Fig. 4A,B). Compressive deformation of the PEG microconstructs across the array was repeatable and ranged from 6.02 ± 0.80% to 25.54 ± 1.52%. (Fig. 4C).

3.3. Cell deformation

Cells encapsulated within the polymerized microconstructs remained rounded after 1 h of incubation. They were evenly dispersed throughout the PEG matrix, but there was some indication of cell settling towards the bottom of the microconstructs during the alignment and polymerization procedure. Cellular deformation (as defined in Section 2.7) was found to increase non-linearly with increasing levels of compression (Fig. 5F). The largest applied compression caused a significant cellular deformation ($p < 0.001$), but all other deformations across the array were not different ($p > 0.269$). Nuclear deformation (Fig. 5G) in response to the applied compressive strains was not significantly different under any of the tested mechanical conditions ($p > 0.121$).

3.4. Parametric finite element simulations

In order to gain a better understanding of the reasons for the observed non-linear relationship between matrix compression and cellular deformation, parametric finite element simulations were conducted. These simulation results (Fig. 6) suggest that the ratio between Young's modulus of the cell and that of the surrounding matrix significantly impacts cellular deformation in a compressed matrix, and this effect is more dramatic at higher strain levels. Cellular

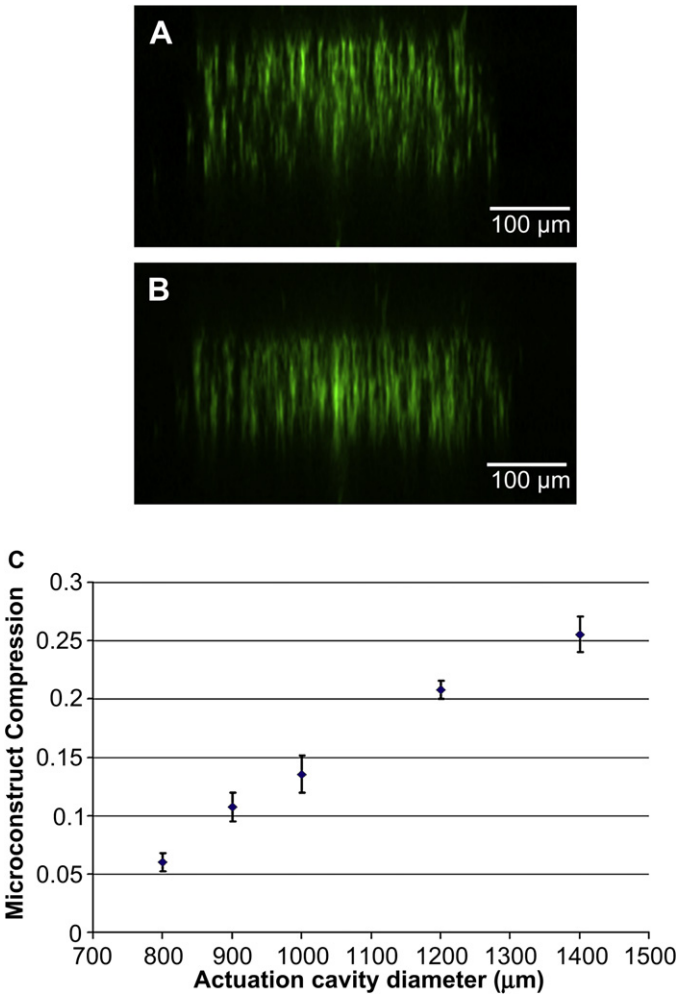

Fig. 4. Characterization of hydrogel compression across the microfabricated array. (A) Orthogonally resliced confocal image of fluorescent bead markers within a single hydrogel cylinder over a unit on the array at rest and (B) when actuated at 55 kPa. (C) Nominal compression means achieved across a 5×5 array of hydrogel cylinders (means $\pm$ standard deviation; $n = 3$).

deformations are small when a cell is encapsulated in a relatively soft hydrogel, but increase as the modulus of the matrix approaches that of the cell. Further increases in matrix stiffness continue to affect cellular deformation, but the impact becomes noticeably smaller when the matrix is an order of magnitude stiffer than the cell.

4. Discussion

The ability to understand cellular response to factors in the microenvironment has been significantly improved by the availability of various technologies. Advances in HTS techniques have enabled rapid screening for the effects of a large number of chemical cues on cellular function, an approach critical to drug discovery, tissue engineering, and probing fundamental cell biology. However, most HTS assays are conducted on static tissue culture plastic, which does not reflect the complexity of *in vivo* systems. Mechanical stimulation and three-dimensional culture conditions are two factors that are known to modulate cellular response to other microenvironmental conditions, but remain unaccounted for in HTS techniques. Hence, there is a need to conduct high-throughput experiments in conditions that capture more of the complexities that define the cellular microenvironment. To address this issue, we have developed a technology that enables high-throughput mechanical compression of cells in a three-dimensional culture system.

Developing this system required the integration of aligned, micropatterned cell-laden biomaterial arrays into multilayer PDMS devices. PEG was chosen as a model biomaterial to demonstrate this technology because of the established use of PEG as a photopatternable biomaterial for encapsulated cell studies [40,42,43]. The ability to comprehensively modify this biomaterial with adhesive ligands [44], establish chemical gradients [45], incorporate degradable crosslinking structures [46,47], and control mechanical stiffness [48] makes PEG particularly suited to this application. Long-term culture of encapsulated cells has been demonstrated [49], and the use of chemical modifications to the hydrogel polymer has shown significantly improved cell behaviour in terms of viability and maintaining regular function [37].

Integrating micropatterned PEG microconstructs into these multilayer PDMS devices was challenging. Incorporation of three-dimensional biomaterials into microfabricated devices has been achieved by assembling the microdevice around the patterned material [50], and by designing 'open-top' microfluidic devices [51]. However, the physical constraints of the present compression system necessitated *in situ* patterned photopolymerization within a closed microfluidic system. Photopolymerization of immobile PEG structures is most often carried out in glass chambers [37,40,42], and though Liu et al. have reported encapsulation of cells within PDMS-glass microchannels, but only for small hydrogel microconstructs (<50 μm diameter) [52]. In the polymerized arrays reported here, each hydrogel was 500 μm in diameter, in order to maximize the matrix volume unaffected by edge-related changes in local strain, and to obtain an adequate number of cells in each microconstruct for analysis.

Current techniques to integrate photopolymerized PEG into PDMS devices [52] do not scale well to 500 μm diameter features. We experimentally found that the polymerization time required to accurately define the hydrogel features in a PDMS-based polymerization chamber was in excess of the cytotoxicity threshold for C3H10T1/2 cells. This is because the polymerization process is quenched by oxygen, and the high oxygen-permeability of PDMS prevents polymerization, while maintaining an increased concentration of toxic photo-generated free radicals. Temporarily depleting the oxygen levels in the PDMS by vacuum treatment improved polymerization times. However, this method was inconsistent, as variations in the time required to align the photomask with the PDMS device created differently sized structures in different devices. To address this problem, the PDMS device was coated with a 1 μm thick layer of Parylene-C. Parylene-C is biocompatible [53] and the gas permeability of a PDMS-Parylene-C composite is substantially lower than PDMS alone [54]. This approach is broadly applicable, and would enable the integration of cell-laden biomaterial arrays into most PDMS device designs.

There are a number of advantages in developing microfabricated platforms to study the effects of mechanical forces on systems. Some of the generic advantages are the minimized use of culture and immunostaining reagents; the ability to generate a large number of experimental conditions without manual intervention; the ability to work with small cell numbers; miniaturized equipment footprints; and reduced cost. Furthermore, the use of this system yields a specific advantage over current macroscale equipment. Compressive stimulation of cells is often accompanied by a transient increase in fluid pressure, which has been shown to impact cell function [55], as a 'side effect' of applying mechanical deformation [56]. Microfabricated constructs have a substantially higher surface to volume ratio than their macroscale counterparts, and hence the transient imbalance in fluid pressure reaches equilibrium more rapidly. Hence, these microfabricated arrays can be

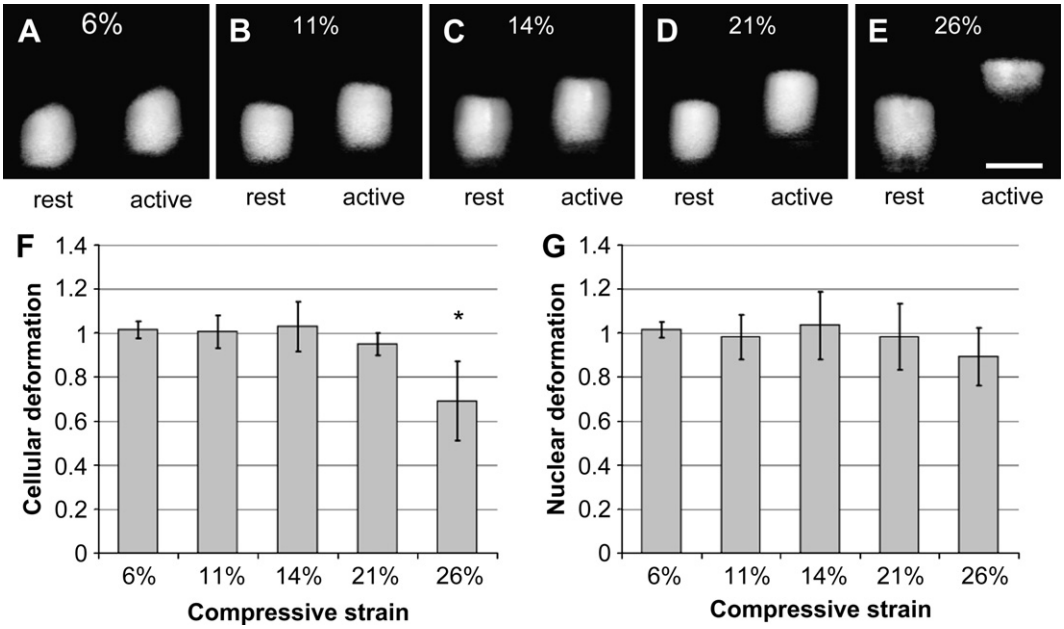

Fig. 5. Deformation of single cells within a compressed matrix. (A–E) Orthogonally resliced confocal images of single cells encapsulated in matrices undergoing increasing levels of compression (scale bar = 20 μm). (F) Cellular deformation observed across the array. Whole cell deformation increases non-linearly with increasing compressive strains (*$p < 0.001$ as compared to all other compression levels). (G) Nuclear deformation observed across the array. No significant changes in nuclear shape were observed at these strain levels.

used to probe cellular response to mechanical compression while minimizing other confounding factors.

As a first demonstration of the mechanically active biomaterial array, cellular and nuclear deformation was assessed in response to matrix compressive strains ranging from 6 to 26%. These hydrogel strains were not translated linearly to encapsulated cells. Nuclear deformation was not significantly different regardless of applied mechanical strain, and cellular deformation only changed significantly at the highest strain levels. We hypothesize that the lack of cellular deformation at lower strain levels was due to the relatively low stiffness of the matrix, compared to the stiffness of the encapsulated cell. At higher strains, the pores in the PEG material collapse, increasing the effective modulus of the matrix [57,58] and causing increased cell deformation. To further explore this hypothesis, first-order linear finite element simulations of cell deformation were conducted in which the relative differences in mechanical stiffness between the cell and the surrounding matrix were varied. The simulation results indicate that within a range of E^*_{matrix}, an increase in matrix stiffness can cause substantial changes in cell deformation for the same applied compression. This effect, similar to that reported by Guilak and Mow [56] for cartilage, supports the hypothesis that cellular deformation is impacted by the non-linear behaviour of the matrix and its stiffness relative to that of the cell.

Though an accurate determination of the relative stiffness difference between the cells and the matrix (E^*_{matrix}) is difficult, a rough estimate can be made. Compressing fibroblasts by micromanipulation suggests a Young's modulus range from 0.1 to 10 kPa [59], and formulations of PEG hydrogels similar to those used in this work have a Young's modulus of 0.1 to 1 kPa [58]. Hence, a rough estimate for E^*_{matrix} at low compressive strains ranges from 0.01 to 1. The finite element simulations indicate that there is little change in cell deformation for all simulated hydrogel compressions in the lower end of this range of E^*_{matrix}. At the upper end of this range however, cell deformations become more substantial. Since PEG has been shown to stiffen at the higher compressive strains tested [58], it is plausible that strain stiffening at higher applied strains increases E^*_{matrix} enough to cause a large increase in cellular deformation.

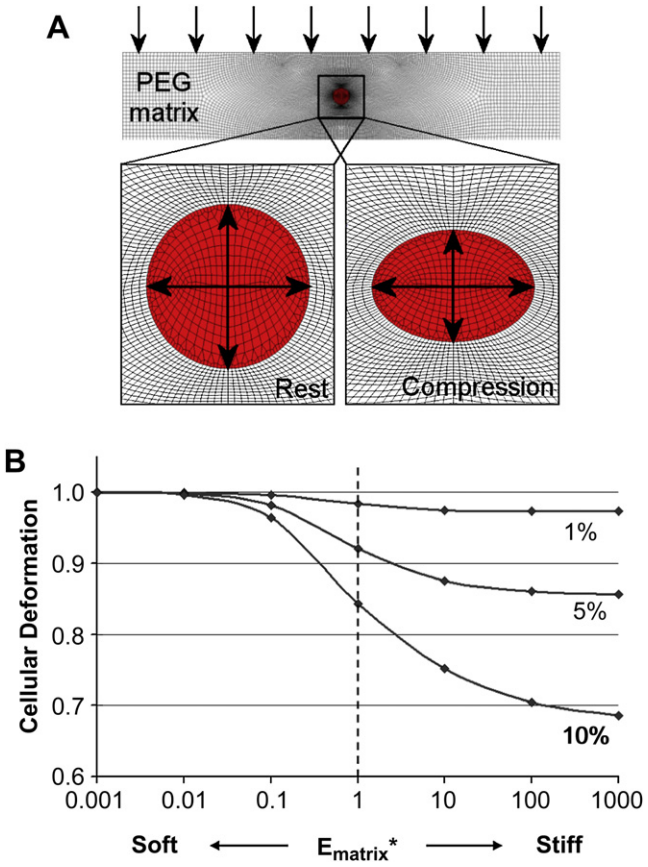

Fig. 6. (A) Finite element simulations showing encapsulated cellular deformation in response to compression of the surrounding matrix. (B) Simulated cellular deformation for 1, 5 and 10% compression in the surrounding matrix, for a range of matrix stiffness properties normalized to the cell stiffness (E^*_{matrix}).

Hence, this model of cell-biomaterial mechanical interaction may explain the non-linear cellular deformation results observed in the compression array. A similar argument applies to the low levels of nuclear deformation observed: the nucleus is three to four times stiffer than the cytoplasm [60], and hence is 'shielded' by the softer surrounding matrix. The observed complex interaction between cell and biomaterial further emphasizes the need for high-throughput approaches to experiments involving mechanical stimulation, particularly when viewed in combination with the number of other microenvironmental parameters that can be varied.

Since the PDMS base platform of the microfabricated array is constructed using standard soft lithography techniques, simple modifications can further extend the utility of this platform technology. Hydrogels with several different chemistries can be formed on a single chip [61], or microfluidic gradient generators could be used with the PEG precursor chemicals, to create a polymerized array with a range of mechanical and chemical properties [62]. The ability to integrate PEG structures into microchannels also enables the delivery of chemical cues in a high-throughput, automated fashion using well-established techniques [3]. Hence, this technology promises rapid assessment of the integrated response of encapsulated cells to mechanical stimulation in combination with a multitude of other factors including hydrogel stiffness, matrix ligand density, hydrogel chemistry, and biochemical cues.

5. Conclusions

Mesenchymal stem cells encapsulated in an array of PEG microconstructs were successfully integrated into an active multilayer PDMS device. Using this system, mechanical compressive strains ranging from 6 to 26% can simultaneously be applied to sections of the array. As a first demonstration of the capabilities of this platform for mechanically active cell culture, nuclear and cellular deformation was assessed in response to various compressive strains. Finite element simulations suggest that the non-linear cellular and nuclear deformations arise from relative differences in the mechanical stiffness of the cell and the surrounding matrix. This information can be used to guide experimental study design in cellular response to compressive stimulation. More broadly, this platform enables HTS of cellular response in three-dimensional environments under combinatorially manipulated mechanobiological conditions. This approach may aid in the development of complex biomaterials and tissue engineering systems and in testing drugs in more physiologically-relevant environments.

Acknowledgements

We thank Morakot Likhitpanichkul and Mohamed Abdelgawad for helpful suggestions and advice, and Christopher Yip and Gary Mo from the Centre for Studies in Molecular Imaging for microscopy expertise and use of equipment. We acknowledge microfabrication support from the Emerging Communications Technology Institute and the Toronto Microfluidics Foundry. We acknowledge financial support from the Natural Sciences and Engineering Research Council of Canada and the Canadian Institutes of Health Research (CHRPJ 323533-06), the Ontario Graduate Scholarship program to CM, and the Canada Research Chairs in Micro and Nano Engineering Systems to YS, and in Mechanobiology to CAS.

Appendix

Figures with essential colour discrimination. Figs. 1, 4 and 6 of this article are difficult to interpret in black and white. The full colour images can be found in the on-line version, at doi:10.1016/j.biomaterials.2009.09.068.

References

[1] Bajorath J. Integration of virtual and high-throughput screening. Nature reviews 2002;1(11):882–94.
[2] Abbott A. Cell culture: biology's new dimension. Nature 2003;424(6951):870–2.
[3] Gomez-Sjoberg R, Leyrat AA, Pirone DM, Chen CS, Quake SR. Versatile, fully automated, microfluidic cell culture system. Analytical Chemistry 2007;79(22):8557–63.
[4] Flaim CJ, Chien S, Bhatia SN. An extracellular matrix microarray for probing cellular differentiation. Nature Methods 2005;2(2):119–25.
[5] Flaim CJ, Teng D, Chien S, Bhatia SN. Combinatorial signaling microenvironments for studying stem cell fate. Stem Cells and Development 2008;17(1):29–39.
[6] Zaari N, Rajagopalan P, Kim SK, Engler AJ, Wong JY. Photopolymerization in microfluidic gradient generators: Microscale control of substrate compliance to manipulate cell response. Advanced Materials 2004;16(23–24):2133.
[7] Anderson DG, Putnam D, Lavik EB, Mahmood TA, Langer R. Biomaterial microarrays: rapid, microscale screening of polymer-cell interaction. Biomaterials 2005;26(23):4892–7.
[8] Yamada KM, Cukierman E. Modeling tissue morphogenesis and cancer in 3D. Cell. 2007;130(4):601–10.
[9] Cukierman E, Pankov R, Stevens DR, Yamada KM. Taking cell-matrix adhesions to the third dimension. Science 2001;294(5547):1708–12.
[10] Griffith LG, Naughton G. Tissue engineering – current challenges and expanding opportunities. Science 2002;295(5557):1009–14.
[11] Griffith LG, Swartz MA. Capturing complex 3D tissue physiology in vitro. Nature Reviews Molecular Cell Biology 2006;7(3):211–24.
[12] Weaver VM, Petersen OW, Wang F, Larabell CA, Briand P, Damsky C, et al. Reversion of the malignant phenotype of human breast cells in three-dimensional culture and in vivo by integrin blocking antibodies. Journal of Cell Biology 1997;137(1):231–45.
[13] Smalley KSM, Lioni M, Herlyn M. Life isn't flat: taking cancer biology to the next dimension. In Vitro Cellular & Developmental Biology-Animal 2006;42(8–9):242–7.
[14] Hwang NS, Kim MS, Sampattavanich S, Baek JH, Zhang ZJ, Elisseeff J. Effects of three-dimensional culture and growth factors on the chondrogenic differentiation of murine embryonic stem cells. Stem Cells 2006;24(2):284–91.
[15] Kunz-Schughart LA, Freyer JP, Hofstaedter F, Ebner R. The use of 3-D cultures for high-throughput screening: the multicellular spheroid model. Journal of Biomolecular Screening 2004;9(4):273–85.
[16] Nguyen KT, West JL. Photopolymerizable hydrogels for tissue engineering applications. Biomaterials 2002;23(22):4307–14.
[17] Khademhosseini A, Langer R. Microengineered hydrogels for tissue engineering. Biomaterials 2007;28(34):5087–92.
[18] Tsang VL, Bhatia SN. Three-dimensional tissue fabrication. Advanced Drug Delivery Reviews 2004;56(11):1635–47.
[19] Jongpaiboonkit L, King WJ, Lyons GE, Paguirigan AL, Warrick JW, Beebe DJ, et al. An adaptable hydrogel array format for 3-dimensional cell culture and analysis. Biomaterials 2008;29(23):3346–56.
[20] Jongpaiboonkit L, King WJ, Murphy WL. Screening for 3D Environments that support human mesenchymal stem cell viability using hydrogel arrays. Tissue Engineering Part A 2009;15(2):343–53.
[21] Simmons CA, Grant GR, Manduchi E, Davies PF. Spatial heterogeneity of endothelial phenotypes correlates with side-specific vulnerability to calcification in normal porcine aortic valves. Circulation Research 2005;96(7):792–9.
[22] Ehrlich PJ, Lanyon LE. Mechanical strain and bone cell function: a review. Osteoporosis International 2002;13(9):688–700.
[23] Wang JH, Thampatty BP. An introductory review of cell mechanobiology. Biomechanics and Modeling in Mechanobiology 2006;5(1):1–16.
[24] Pedersen JA, Swartz MA. Mechanobiology in the third dimension. Annals of biomedical engineering 2005;33(11):1469–90.
[25] MacKenna DA, Dolfi F, Vuori K, Ruoslahti E. Extracellular signal-regulated kinase and c-Jun NH2-terminal kinase activation by mechanical stretch is integrin-dependent and matrix-specific in rat cardiac fibroblasts. The Journal of Clinical Investigation 1998;101(2):301–10.
[26] Lee WC, Maul TM, Vorp DA, Rubin JP, Marra KG. Effects of uniaxial cyclic strain on adipose-derived stem cell morphology, proliferation, and differentiation. Biomechanics and Modeling in Mechanobiology 2007;6(4):265–73.
[27] McBeath R, Pirone DM, Nelson CM, Bhadriraju K, Chen CS. Cell shape, cytoskeletal tension, and RhoA regulate stem cell lineage commitment. Developmental Cell 2004;6(4):483–95.
[28] Burdick JA, Vunjak-Novakovic G. Engineered microenvironments for controlled stem cell differentiation. Tissue Engineering Part A 2009;15(2):205–19.
[29] Loening AM, James IE, Levenston ME, Badger AM, Frank EH, Kurz B, et al. Injurious mechanical compression of bovine articular cartilage induces chondrocyte apoptosis. Archives of Biochemistry and Biophysics 2000;381(2):205–12.
[30] Buschmann MD, Gluzband YA, Grodzinsky AJ, Hunziker EB. Mechanical Compression Modulates Matrix Biosynthesis in Chondrocyte Agarose Culture. Journal of Cell Science 1995;108:1497–508.

[31] Wang DL, Jiang SD, Dai LY. Biologic response of the intervertebral disc to static and dynamic compression in vitro. Spine 2007;32(23):2521–8.
[32] Robling AG, Niziolek PJ, Baldridge LA, Condon KW, Allen MR, Alam I, et al. Mechanical stimulation of bone in vivo reduces osteocyte expression of Sost/sclerostin. Journal of Biological Chemistry 2008;283(9):5866–75.
[33] Pelaez D, Huang CYC, Cheung HS. Cyclic compression maintains viability and induces chondrogenesis of human mesenchymal stem cells in fibrin gel scaffolds. Stem Cells and Development 2009;18(1):93–102.
[34] Rath B, Nam J, Knobloch TJ, Lannutti JJ, Agarwal S. Compressive forces induce osteogenic gene expression in calvarial osteoblasts. Journal of Biomechanics 2008;41(5):1095–103.
[35] Yanagisawa M, Suzuki N, Mitsui N, Koyama Y, Otsuka K, Shimizu N. Effects of compressive force on the differentiation of pluripotent mesenchymal cells. Life Sciences 2007;81(5):405–12.
[36] Mauck RL, Nicoll SB, Seyhan SL, Ateshian GA, Hung CT. Synergistic action of growth factors and dynamic loading for articular cartilage tissue engineering. Tissue Engineering 2003;9(4):597–611.
[37] Tsang VL, Chen AA, Cho LM, Jadin KD, Sah RL, DeLong S, et al. Fabrication of 3D hepatic tissues by additive photopatterning of cellular hydrogels. FASEB Journal 2007;21(3):790–801.
[38] Jo BH, Van Lerberghe LM, Motsegood KM, Beebe DJ. Three-dimensional microchannel fabrication in polydimethylsiloxane (PDMS) elastomer. Journal of microelectromechanical systems 2000;9(1):76–81.
[39] Moraes C, Sun Y, Simmons CA. Solving the shrinkage-induced PDMS alignment registration issue in multilayer soft lithography. Journal of micromechanics and microengineering 2009;19(6):065015.
[40] Liu VA, Bhatia SN. Three-dimensional photopatterning of hydrogels containing living cells. Biomedical microdevices 2002;4(4):257–66.
[41] Panda P, Ali S, Lo E, Chung BG, Hatton TA, Khademhosseini A, et al. Stop-flow lithography to generate cell-laden microgel particles. Lab on a chip 2008;8(7):1056–61.
[42] Hahn MS, Taite LJ, Moon JJ, Rowland MC, Ruffino KA, West JL. Photolithographic patterning of polyethylene glycol hydrogels. Biomaterials 2006;27(12):2519–24.
[43] Albrecht DR, Tsang VL, Sah RL, Bhatia SN. Photo- and electropatterning of hydrogel-encapsulated living cell arrays. Lab on a chip 2005;5(1):111–8.
[44] Roberts MJ, Bentley MD, Harris JM. Chemistry for peptide and protein PEGylation. Advanced Drug Delivery Reviews 2002;54(4):459–76.
[45] DeLong SA, Moon JJ, West JL. Covalently immobilized gradients of bFGF on hydrogel scaffolds for directed cell migration. Biomaterials 2005;26(16):3227–34.
[46] Lee SH, Miller JS, Moon JJ, West JL. Proteolytically degradable hydrogels with a fluorogenic substrate for studies of cellular proteolytic activity and migration. Biotechnology Progress 2005;21(6):1736–41.
[47] Kloxin AM, Kasko AM, Salinas CN, Anseth KS. Photodegradable hydrogels for dynamic tuning of physical and chemical properties. Science 2009;324(5923):59–63.
[48] Peyton SR, Raub CB, Keschrumrus VP, Putnam AJ. The use of poly(ethylene glycol) hydrogels to investigate the impact of ECM chemistry and mechanics on smooth muscle cells. Biomaterials 2006;27(28):4881–93.
[49] Weber LM, He J, Bradley B, Haskins K, Anseth KS. PEG-based hydrogels as an in vitro encapsulation platform for testing controlled beta-cell microenvironments. Acta Biomaterialia 2006;2(1):1–8.
[50] Khademhosseini A, Yeh J, Jon S, Eng G, Suh KY, Burdick JA, et al. Molded polyethylene glycol microstructures for capturing cells within microfluidic channels. Lab on a chip 2004;4(5):425–30.
[51] Figallo E, Cannizzaro C, Gerecht S, Burdick JA, Langer R, Elvassore N, et al. Micro-bioreactor array for controlling cellular microenvironments. Lab on a chip 2007;7(6):710–9.
[52] Liu J, Gao D, Li HF, Lin JM. Controlled photopolymerization of hydrogel microstructures inside microchannels for bioassays. Lab on a chip 2009;9(9):1301–5.
[53] Chang TY, Yadav VG, De Leo S, Mohedas A, Rajalingam B, Chen CL, et al. Cell and protein compatibility of parylene-C surfaces. Langmuir 2007;23(23):11718–25.
[54] Mehta G, Lee J, Cha W, Tung YC, Linderman JJ, Takayama S. Hard top soft bottom microfluidic devices for cell culture and chemical analysis. Analytical chemistry 2009;81(10):3714–22.
[55] Sim WY, Park SW, Park SH, Min BH, Park SR, Yang SS. A pneumatic micro cell chip for the differentiation of human mesenchymal stem cells under mechanical stimulation. Lab on a chip 2007;7(12):1775–82.
[56] Guilak F, Mow VC. The mechanical environment of the chondrocyte: a biphasic finite element model of cell–matrix interactions in articular cartilage. Journal of biomechanics 2000;33(12):1663–73.
[57] Lee SY, Pereira BP, Yusof N, Selvaratnam L, Yu Z, Abbas AA, et al. Unconfined compression properties of a porous poly(vinyl alcohol)-chitosan-based hydrogel after hydration. Acta Biomaterialia 2009;5(6):1919–25.
[58] Almany L, Seliktar D. Biosynthetic hydrogel scaffolds made from fibrinogen and polyethylene glycol for 3D cell cultures. Biomaterials 2005;26(15):2467–77.
[59] Ethier CR, Simmons CA. Introductory biomechanics: from cells to organisms. Cambridge University Press; 2007.
[60] Guilak F, Tedrow JR, Burgkart R. Viscoelastic properties of the cell nucleus. Biochemical and biophysical research communications 2000;269(3):781–6.
[61] Huang CP, Lu J, Seon H, Lee AP, Flanagan LA, Kim HY, et al. Engineering microscale cellular niches for three-dimensional multicellular co-cultures. Lab on a chip 2009;9(12):1740–8.
[62] Burdick JA, Khademhosseini A, Langer R. Fabrication of gradient hydrogels using a microfluidics/photopolymerization process. Langmuir 2004;20(13):5153–6.